Chapter 7

Feedback Control Techniques for the Mechanistic Analysis of Electrochemical Systems

7.1 Introduction

In the chemical engineering literature, both classical Proportional-Integral-Derivative (PID) and modern nonlinear feedback control methods have frequently been studied where a chemical process was to follow a prescribed behavior [100, 107]. PID methods, in particular, have been described for the manipulation of the stability of stationary states, sustained oscillations or chaotic regimes in chemical systems [99, 199, 200, 201, 202, 105, 203]. However, the number of experimental studies using pure derivative feedback control is very limited [105] and focus was primarily placed on the stabilization of unstable states. The use of feedback control as a tool in the mechanistic analysis of chemical systems is a novel concept and has never been discussed so far in literature. Especially in electrochemical systems the control parameters current I and potential U are easily accessible and therefore allow a fast implementation of feedback experiments. Two challenging problems associated with the mechanistic analysis of electrochemical systems will be addressed here: First, the identification of "truly potentiostatic" oscillators and, second, the distinction between different subcategories with the group of HNDR oscillators.

As outlined in chapter 2, apart from electrochemical instabilities based on negative impedance whether or not visible on the stationary polarization curve (NDR and HNDR, respectively), there are "truly potentiostatic" oscillatory models [74] where the source of the instability is of purely chemical nature, e.g. due to a chemical autocatalysis or to an adsorbate interaction. The term "truly potentiostatic" is justified only in the limiting case of negligible ohmic potential drop between working and reference electrode since under these conditions the double layer potential equals the constant outer applied potential U_{ex} despite of sustained current oscillations. Note that at higher values of the ohmic resistance, ϕ oscillates even if it is nonessential for the dynamics. There are a few experimental systems which are believed to fall into

this class but clear evidence for the purely chemical nature of their instabiliy is still missing [76, 67, 77, 78]

The only experimental test, so far, in order to find out whether or not an experimental oscillator is truly potentiostatic consists in the measurement of the I/U behavior for vanishing ohmic potential drop by means of electronic IR compensation or very high solution conductivities. If there are current oscillations for completely compensated or negligible resistance, the instability must be of purely chemical nature and ϕ is proved to be nonessential. Otherwise the ohmic drop is crucial for oscillations and ϕ is an essential variable. However, numerous experimental studies revealed to be ambiguous since it often turned out very difficult to decide whether the effect of an ohmic resistance could be completely ruled out. The electronic compensation method, on the other hand, requires the precise knowledge of the ohmic resistance to be compensated.

The studies by Koper [64] and Wolf [29] as well as the results from chapters 4 and 5 [72] revealed that the HNDR category can be generally subdivided into two different subcategories depending whether

- there is a fast third chemical species (e.g. Cl^- or OH for the H_2 and FA oxidation system) involved in the positive feedback loop (negative impedance) with the major current-providing reaction (hydrogen oxidation, direct formic acid oxidation path in suboscillator 1) not consuming the slow chemical species

or whether

- the major current-providing process does consume the slow chemical species, may it be a volume or surface species, and there is a potential-dependent supply (electrosorption etc.) of this species [64].

In any case, as already noted by Koper in ref. [74], at least two potential-dependent processes must be present in an electrochemical oscillator of the HNDR type. Although frequency response techniques have proven to be extremely useful for the prediction of bifurcations, a distinction between these subcategories based on the impedance spectrum is impossible.

It is the purpose of this chapter to introduce and to investigate two derivative feedback control tests both experimentally and theoretically which will be shown to provide useful mechanistic information on unknown electrochemical oscillators. After the experimental details (section 2), section 3 introduces the first control method which is shown to allow the identification of a truly potentiostatic oscillator without explicit knowledge of the ohmic resistance. In section 4, the second control test is shown to be a tool for an experimental distinction between the two different oscillatory mechanisms within the HNDR category. The discussion in section 5, finally, summarizes the results and assesses both methods regarding their advantages and drawbacks.

7.2 Experimental

A rotating Au-ring-Pt-disc electrode, a Pt wire and a Hg_2SO_4-electrode with Luggin capillary served as working, counter and reference electrodes, respectively. The reference electrode of the potential values reported are either the Standard Calomel Electrode (SCE) or the Hg_2SO_4 electrode and are indicated in the figures and text. The working electrode had an area of 0.125 cm^2. All solutions were prepared with tridistilled water, H_2SO_4 was of suprapure grade.

$\frac{dI}{dt}/U$ control. The continuous feedback control which feeds the time derivative of the instantaneous total current back onto the applied potential is henceforth called $\dot{I}/U$- derivative control. This control was applied to the H_2 oxidation in the presence of copper and chloride ions as well as to the FA oxidation system. All experiments were performed under potentiostatic conditions with an appropriate external ohmic resistance put in series to the electrochemical cell in order to obtain stable current oscillations [26, 98, 72]. The Au-ring electrode was not used in these experiments.

$\dot{\theta}/I$-control. The continuous time derivative feedback control between the fractional surface coverage of a chemical species, θ, and the total current was applied to the oscillatory galvanostatic H_2 oxidation system in the presence of Cu^{2+} and Br^-, since in contrast to the formic acid system, the time derivative of the coverages of the species involved were conveniently measurable at the Au ring electrode.

H_2-oxidation system

Before the experiments, cyclic voltammograms in 0.5 mol/l H_2SO_4 (N_2-saturated) were recorded in order to test the Pt-poly-disc and to achieve a stable, reproducible I/U behavior. Thereafter, appropriate quantities of solutions of $CuSO_4$ and HBr or HCl were added to the bulk electrolyte. All chemicals were of suprapure grade.The electrolyte was kept under a H_2 atmosphere (5N). Continuous stirring (2000 rpm) ensured sufficient mass-transport of H_2 to the Pt-disc required for sustained current oscillations. After addition of an external ohmic resistance (R_{ex}=3 kΩ for potentiostatic control, 7 kΩ prior to galvanostatic control) between working electrode and potentiostat, sustained current oscillations emerged. Prior to $\dot{\theta}/I$-control experiments, the system conditions were switched to galvanostatic operation at currents where sustained potential oscillations occurred. For further details on the experimental system see ref. [26, 75].

Formic acid oxidation system

Two different solutions (1 mol/l sodium formiate, HCOONa p.a., in 0.5 mol/l H_2SO_4 and 3 mol/l NaOOCH in 1mol/l H_2SO_4) were used for experiments. As before, the electrolyte was purged by 5N N_2 to remove dissolved oxygen. An external ohmic resistance (R_{ex}=1 kΩ) was crucial for the observation of sustained current oscillations on the Pt-poly-disc electrode for both solution concentrations. Experimental details on the oscillatory formic acid system can be found in ref. [130, 88, 98].

Experimental implementation of derivative control techniques

For all $\dot{I}/U$ experiments, a home-built potentiostat was used, whereas a bipotentiostat/galvanostat served as power source during the RRDE $\dot{\theta}/I$ control experiments. Both potentiostat and galvanostat were equipped with an external additive input socket for the additive modulation of the applied cell potential (U_{ex}) and the applied total current I, respectively.

$\frac{dI}{dt}/U$ derivative-control. The $\dot{I}/U$-derivative feedback control was implemented by an analog OP amplifyer circuit similar to the one shown in Fig. 6 of ref. [105]. The circuit was used as a feedback between the total current output socket of the potentiostat and its input socket for external additive potentials. The derivative device determined the negative time derivative of the instantaneous total current I, multiplied this quantity by a variable positive gain α (adjustable by means of a variable resistor) and fed the resulting potential signal additively back onto the initially contant applied potential $U_{ex} = U_{ex0}$ through the external additive potential input. After the control has turned on, the previously constant applied potential U_{ex} turns into an additional time dependend variable.

The simple control scheme reads

$$U_{ex}(\alpha, t) = U_{ex0} + \alpha \frac{dI(t)}{dt}$$

$\dot{\theta}/I$-derivative control. The control was implemented by means of the Au ring electrode which served as a probe for the instantaneous value of $\dot{\theta}_{Br^-}$ or $\dot{\theta}_{Cu}$. At a ring potential $U_{ring} = +0.7$ V/Hg_2SO_4 bromide is oxidized to bromine according

$$2Br^- \longrightarrow Br_2 + 2e^-$$

[204, 205], whereas at $U_{ring} = -0.62$ V/Hg_2SO_4 copper ions are reduced according

$$Cu^{2+} + 2e^- \longrightarrow Cu$$

[204]. To see the relation between the ring current and $\dot{\theta}$ recall the relation valid at a RRDE between θ of a chemical species at the disc and the time integral over the deviations of the stationary ring current $\Delta I_{ring} = I_{ring} - I_{ring,0}$; the relation is usually used for the evaluation of θ during potential step experiments and reads

$$\theta \propto c \int \Delta I_{ring} d\tau.$$

Here, the constant c comprises the charge transferred when a monolayer of the chemical species ad- or desorbs as well as a geometry-dependent collection efficiency which takes into account mass losses of the desorbed species. From the given relation it is obvious that the instantaneous value of ΔI_{ring} is proportional to $\dot{\theta}$. The sign of the proportionality factor, however, depends on the nature of the detecting electrochemcial process. For anodic ring processes, like the oxidation of Br^-, there holds the

relation

$$\Delta I_{ring} \propto -\dot{\theta}_{Br^-}, \tag{7.1}$$

whereas a cathodic process like the one used to monitor copper leads to

$$\Delta I_{ring} \propto +\dot{\theta}_{Cu}.$$

This means that a negative feedback requires a positive gain and a negative gain in the case of an anodic and cathodic ring process, respectively.

The instantaneous ring current was digitally read into a PC and then processed online using the given values of $I_{ring,0}$, the stationary ring current, and α, followed by the output of the control signal. This instantaneous evaluation of the control signal occurred with a frequency of 200 Hz. The software allowed a online variation of both parameters.

7.3 $\frac{dI}{dt}/U$-derivative control

7.3.1 Experimental results

Fig. 7-1 shows the effect on the oscillatory current density j in the H_2 oxidation system when the negative time derivative of j is continuously fed back on U_{ex} ($U_{ex0} = 403mV$). At $t = 30s$, the control is switched on using $\alpha = 0.6$. The control signal ΔU, shown in the upper graph of Fig.7-1, shows a strong initial puls followed by periodic oscillations. The strong initial puls is due to the fact that control was switched on the fast negative flank of the current oscillations giving rise to a high value of the time derivative. Upon control, the current oscillations plotted in the lower portion of Fig.7-1, strongly decrease in amplitude, but do not settle on a stable stationary point. This behavior was qualitatively found for all control gains α ranging from almost zero to very large negative values. When the control was switched off ($t = 85s$ and $t = 155s$), the electrochemical system quickly relaxed back to the original limit cycle.

Fig. 7-2 and 7-3 depict the results of derivative control experiments in the formic acid oxidation system for two different concentrations of the electroactive species and applied potential U_{ex}. Again, the control signal exhibits aperiodic behavior. Since a higher gain was chosen, the derivative circuit showed a small potential offset seen by the slight shift of the zero line in the time series of the control signal. This potential offset, however, did not qualitatively affect the experimental result. The current oscillations are seen to decrease in amplitude as well as in period, yet do not die out in favor of the stabilization of a stationary point. Similar behavior under control action was found for all applied control gains over the entire oscillatory potential range. After control had been switched off, the formic acid system slowly relaxed back to the original dynamical regime.

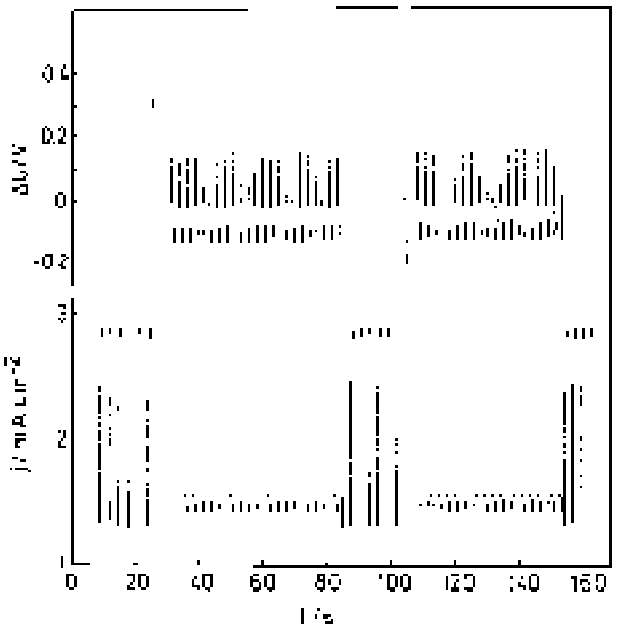

Figure 7-1: Experimental derivative feedback control in the H_2 oxidation system under potentiostatic conditions. The instantaneous derivative of the total current $\dot{I}$ is multiplied by a control gain α, then added to the applied potential U_{ex0} according to $U = U_{ex0} + \alpha \dot{I}$. The upper and lower time series show the time evolution of the applied control signal ΔU and the response in the total current density j. The control was switched on and off at $t = 23s, 105s$ and respectively at $t = 85s, 155s$. Experimental parameters: 10^{-5} mol/l Cu^{2+}; 10^{-4} mol/l Cl^-; 0.5 mol/l H_2SO_4; rotation rate: 3000 rpm; $R_{ex}A = 375\ \Omega\, cm^2$; $U_{ex0} = 403$ mV/SCE; control gain $\alpha = -0.6$.

7.3.2 Model calculations

Consider the simple electrochemical reaction scheme

$$X + * \overset{k_a(\phi), k_d(\phi)}{\rightleftharpoons} X_{ads} \tag{7.2}$$

$$Z + * \overset{k_r(\phi)}{\longrightarrow} P + ne^- \tag{7.3}$$

where X, Z,$*$ and P denote two electroactive species (subscript 'ads' to indicate the adsorbed state), a free surface site and an inert oxidation product, respectively. $k_a(\phi)$, $k_d(\phi)$ and $k_r(\phi)$ represent the ad- and desorption rate constants of X and the rate constant of the current-carrying reaction (7.3), respectively, which are assumed to depend on the instantaneous double layer potential ϕ. Mass transport is assumed to be fast. Therefore, the volume concentrations of the electroactive species

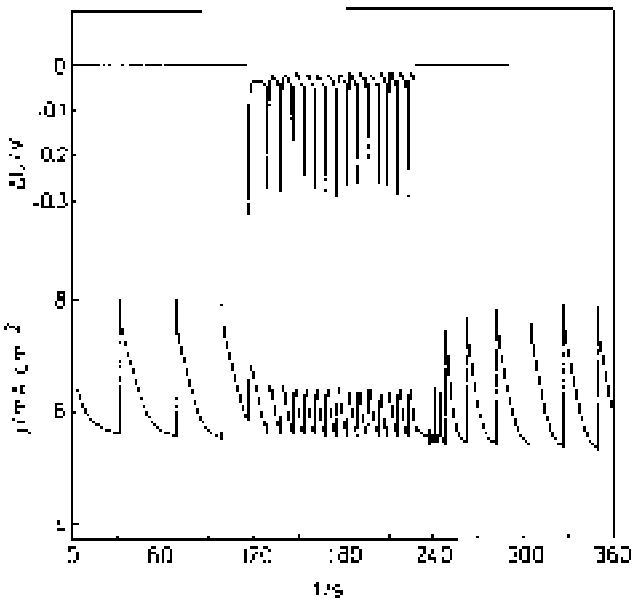

Figure 7-2: Experimental continuous derivative feedback control in the formic acid oxidation system under potentiostatic conditions. Control is implemented as in Fig. **??**. The upper and lower time series show the time evolution of the applied control signal and the response in the total current density j. Experimental parameters: 1 mol/l HCOONa; 0.5 mol/l H_2SO_4; no stirring; $R_{ex}A$= 125 $\Omega\, cm^2$; U_{ex0} = 836 mV/SCE; control gain $\alpha = -7.0$

at the surface equal their bulk values which are considered to be constant in time. Consequently, the concentrations of the volume species become all nonessential for the system dynamics. The electrochemical system is considered under potentiostatic conditions, i.e. at constant applied potential U_{ex}.

Transforming the given reaction scheme into a dimensionless mathematical model of the essential variables θ, the coverage of the X_{ads}, and ϕ, one obtains

$$\dot{\theta} = f(\theta, k_a(\phi), k_d(\phi)) \tag{7.4}$$

$$\epsilon\dot{\phi} = \frac{U_{ex} - \phi}{\rho} - h(\theta, k_r(\phi)) \tag{7.5}$$

with the function f modelling the adsorption and desorption of the chemical species X; the second equation takes care of the overall charge balance of the system with h representing the rate expression of the faradaic current (current carrier). Note that the overall current is provided by the electrochemical oxidation of a nonessential species. The parameters ρ and ϵ denote a dimensionless ohmic resistance (solution

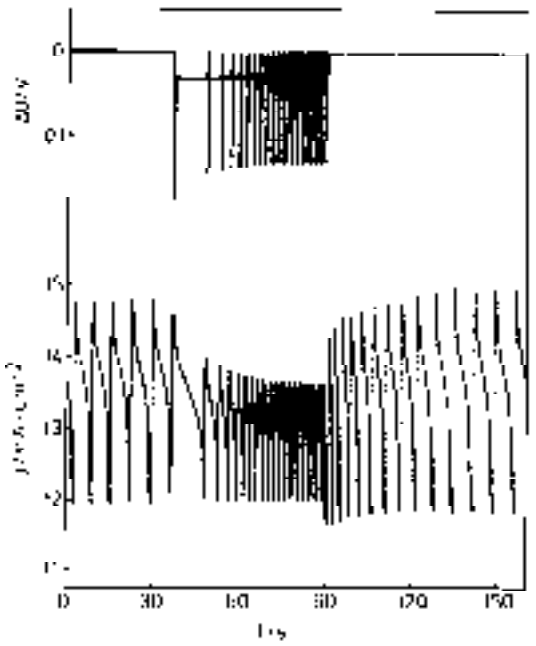

Figure 7-3: Experimental feedback dynamics like in previous figure. Experimental parameters: 3 mol/l HCOONa; 1 mol/l H_2SO_4; no stirring; $R_{ex}A$= 125 $\Omega\, cm^2$; U_{ex0} = 1771 mV/SCE; control gain $\alpha = -5.0$.

as well as external resistance) and a relative time scale of the dynamics of ϕ and θ, respectively. Usually, ϵ is very small which makes ϕ a fast variable.

In order for the model to exhibit the essential mechanistic features of the experimentally investigated systems, h is assumed to show a negative differential resistance [64, 74, 23, 26, 153, 72] over some potential region. This behavior can be due to an additional fast chemical variable [26, 72] (see 3-variable model in section 4) or due to some other (electrochemical) mechanisms such as electrostatic Frumkin repulsion or fast adsorption and desorption of a catalyst [23]. The model exhibits galvanostatic oscillations implying that it belongs to the HNDR category. In the case of an anodic faradaic current ($h > 0$) such as H_2 or FA oxidation the HNDR implies

$$Re\ Z^{-1} = h_\phi + h_\theta \frac{-f_\phi f_\theta}{\omega^2 + f_\theta^2} < 0$$

for a finite perturbation frequency ω, where Z denotes the complex faradaic impedance and the subscripts represent the partial derivatives.

In the vicinity of the stationary steady state (θ_{ss}, ϕ_{ss} with $U_{ex} = U_{ex0}$), the time

evolution of the uncontrolled system can be written as

$$\begin{pmatrix} \dot{\theta\prime} \\ \dot{\phi\prime} \end{pmatrix} = \begin{pmatrix} f_\theta & f_\phi \\ -h_\theta & -h_\phi - \frac{1}{\rho} \end{pmatrix} \begin{pmatrix} \theta\prime \\ \phi\prime \end{pmatrix} + \begin{pmatrix} 0 \\ \frac{1}{\rho} \end{pmatrix} u\prime \tag{7.6}$$

$$= J_{2\times 2} \begin{pmatrix} \theta\prime \\ \phi\prime \end{pmatrix} + Bu\prime \tag{7.7}$$

with the perturbation variables $u\prime = U_{ex} - U_{ex0} = 0; \theta\prime = \theta - \theta_{ss}; \phi\prime = \phi - \phi_{ss}$. $J_{2\times 2}$ denotes the 2×2-Jacobian of the model. The functional expression with a variable as subscript symbolize the first derivative with respect to the subscript variable evaluated at the stationary state $(\theta_{ss}, \phi_{ss}, U_{ex0})$.

For the further analysis, it is assumed that the functional forms of f and h (Butler-Volmer- type expressions) as well as the kinetic parameters are chosen such that the model exhibits stable current oscillations beyond a Hopf bifurcation. This implies $f_\theta < 0$, $f_\phi < 0$ as well as that both the determinant ($DetJ_{2\times 2}$) and the trace of the system Jacobian ($TrJ_{2\times 2}$) are positive.

Implementation of $\frac{dI}{dt}/U$ derivative feedback control

The derivation of the mathematical formulation of derivative control is straightforward [105]. The expression for the instantaneous, small parameter changes δU_{ex} reads

$$\delta U_{ex}(\alpha, t) = U_{ex}(\alpha, t) - U_{ex0} \tag{7.8}$$

$$= \alpha \frac{dj(t)}{dt} \tag{7.9}$$

$$= \alpha \frac{\dot{U}_{ex}(\alpha, t) - \dot{\phi}}{\rho} \tag{7.10}$$

After rearrangement one obtains

$$\dot{U}_{ex}(\alpha, t) = \frac{\rho}{\alpha}(U_{ex} - U_{ex0}) + \dot{\phi} \tag{7.11}$$

Under control conditions the original equations 7.4 and 7.5 as well as eq. 7.11 have to be integrated simultaneously. From eq. 7.11 it is seen that the control creates the additional system variable (U_{ex}) and turns the resulting system into a three-variable system.

Linear stability analysis in the time domain

The evaluation of the eigenvalues λ_i of the three-variable system leads to the characteristic third-order polynom

$$\lambda^3 + a\lambda^2 + b\lambda + c = 0 \tag{7.12}$$

with

$$a = -TrJ_{3\times3} = -(TrJ_{2\times2} + \frac{1}{\epsilon\rho} + \frac{\rho}{\alpha}) \tag{7.13}$$

$$b = \sum |J_{ij}| = DetJ_{2\times2} + \frac{\rho}{\alpha}TrJ_{2\times2} + \frac{f_\theta}{\epsilon\rho} \tag{7.14}$$

$$c = -DetJ_{3\times3} = -DetJ_{2\times2}\frac{\rho}{\alpha} \tag{7.15}$$

Here, the expression $|J_{ij}|$ symbolizes the determinant of the submatrix which is obtained from $J_{3\times3}$ by cancelling the ith row and the jth column.

From eq. 7.13-7.15 the controlled system is seen to exhibit the following dynamics in dependence of α:

a) $\alpha \to 0$ with $\alpha < 0 \implies a \to +\infty, b \to -\infty, c \to +\infty$
b) $\alpha \to -\infty \implies a < 0, b \to DetJ_{2\times2} + \frac{f_\theta}{\epsilon\rho}, c \to 0$ with $c > 0$
c) $\alpha \to +\infty \implies a < 0, b \to DetJ_{2\times2} + \frac{f_\theta}{\epsilon\rho}, c \to 0$ with $c < 0$

In case a), the three-variable model essentially transforms back into the original two-variable case with U_{ex} being nonessential. Case b) corresponds to the experimentally applied negative feedback control and is the relevant case for the conclusions concerning the practical applicability of $\dot{I}/U$ derivative feedback control: The stability analysis reveals that parameter c remains positive for all negative gains α, whereas either a or b are negative. Hence, according to the stability condition of third-order polynoms [195] the system dynamics is governed by two complex conjugate with positive real part and one negative real eigenvalue. It follows that by means of a negative derivative feedback control between the total current and the applied potential, the model eq. 7.4, 7.5 cannot be stabilized on the unstable steady state. Note that for increasingly negative α, the current amplitude steadily decreases, the control signal $\delta U_{ex}(\alpha, t)$, however, remains finite indicating the continuing oscillatory nature of the system dynamics. It is obvious that the failure of the control is due to the existence and structure of the evolution equation of ϕ which must be considered whenever ρ is not negligible. In case c, i.e. for a derivative control with positive gain, the value of parameter c is positive at finite α. According to [195], this indicates a divergent behavior of the model dynamics.

Linear stability analysis in the Laplace domain

In control engineering, the stability of open-loop and closed-loop control systems is usually evaluated in the Laplace domain rather than in the time domain. Especially for closed-loop control systems, this method makes stability analyses much easier and more transparent. First, a functional relation between in- and output of the open-loop system, called the open-loop transfer function, is calculated in the Laplace domain. Then, the transfer function of the applied feedback controller (here derivative control) is determined. Both transfer function uniquely determine the characteristic equation and therefore the stability properties of the overall closed-loop control system. For an

illustrative and detailed introduction into the concept of transfer functions of control systems the reader is referred to ref. [107].

Eq. 7.7 constitutes a typical single-input-single-output (SISO) open-loop control system in the time domain whose input control parameter is $u\prime$ and whose single output variable y, is determined by an appropriate row vector C according to the relation .

$$y = C \begin{pmatrix} \theta\prime \\ \phi\prime \end{pmatrix} \quad C = \begin{pmatrix} 0 & 1 \end{pmatrix} \tag{7.16}$$

Here, C is chosen such that the double layer potential $\phi\prime$ is the output of the control system.

From eq.7.7 and 7.16, the open-loop transfer function $H(s)$ can easily be obtained according to $H(s) = CAdj(sI - J_{2\times2})B/(s^2 - TrJ_{2\times2}s + DetJ_{2\times2})$ with s and Adj denoting the Laplace variable and the adjunctive matrix. The transfer function represents the ratio of the Laplace tranforms of the output and the input and completely charaterizes the system's linear response to perturbations in the control parameter (see Fig. 7-4a). For the given system eq. 7.4,7.5 the open-loop transfer function reads

$$H(s) = \frac{\rho^{-1}(s - f_\theta)}{s^2 - TrJ_{2\times2}s + DetJ_{2\times2}}$$

The derivative controller provides the feedback between the output $y = \phi\prime$ and the control parameter $u\prime$ of the system using the time derivatives of $u\prime$ and $\phi\prime$ as input and providing $u\prime$ as output. Analogous to the system, the controller is also characterized by a transfer function $G(s)$, which by inspection from eq. 7.11 is a 'lead-lag controller' and reads

$$G(s) = \frac{s}{s - \rho\alpha^{-1}}.$$

The stability of the overall closed-loop control system (system plus controller, see Fig. 7-4b is characterized by a total transfer function $T(s) = f(H(s), G(s))$. The stability of $T(s)$ is determined by its poles which are the roots of the denominator of $T(s)$ and can be calculated from

$$1 - H(s)G(s) = 0.$$

Although this equation is equivalent to the characteristic equation of the three-variable system in the time-domain (eq. 7.13 - 7.15), the dependence of the eigenvalues on the applied controller is more transparent than in the formulation in the time domain.

Numerical model calculations

A realistic potentiostatic three-variable model of the oscillatory H_2 oxidation in the presence of Cl^- and Cu^{2+} was used in order to check the analytical predictions concerning the effect of $\dot{I}/U$ feedback control on electrochemical system where ϕ is

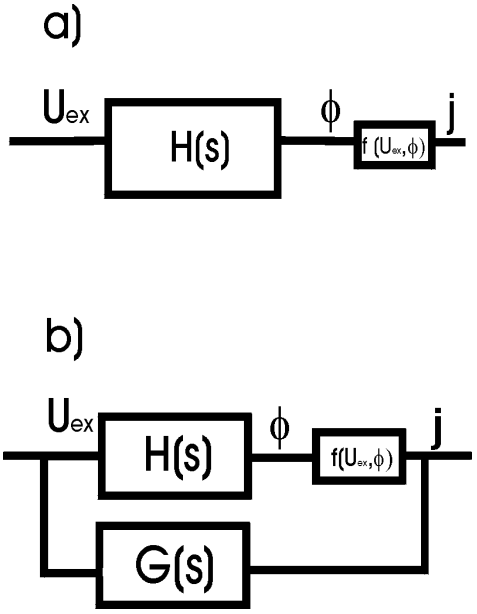

Figure 7-4: a) Schematic representation of an electrochemical open-loop control system with transfer function H(s). The outer potential U and the current density j serve as control parameter and output variable, respectively. b) closed-loop control system with controller transfer function G(s).

an essential variable. The model variables used are θ_{Cu} and θ_{Cl^-} as well as ϕ according to eq. 7.5. A detailed derivation and formulation of the model as well as the values of the kinetic parameters not given in the figure captions can be found in Table 1 of ref. [26] and ref. [29]. The uncontrolled model was modified according to the above control strategy (eq. 7.11).

Fig. 7-5b shows the effect of negative derivative control on the total current j for a parameter set where the system exhibits sustained current oscillations. At $t = 20$ the feedback control was turned on. The system continues to show stable periodic current behavior with smaller amplitude. This behavior remains unchanged for increasing negative values of α. Fig. 7-5a displays the corresponding instantaneous applied control signal ΔU analogous to Fig. 7-1. The model is seen to essentially reproduce the experimental dynamical response.

Furthermore, $\dot{I}/U$ control was implemented in a recently proposed 4-variable model of FA oxidation [72]. The system variables are the concentration of FA at the double layer, the fractional coverage of CO and OH as well as the double layer potential ϕ. Fig. 7-6a and 7-6b display the response of the system upon control. Just as in the H_2 system, the unstable stationary state could not be stabilizied even for very negative values of α. Instead, only small-amplitude oscillations were obtained. Fig. 7-7c and 7-7d show the time evolution of the variable ϕ and U_{ex} under control, respectively. Surprisingly, in contrast to the current j the amplitude of ϕ increased.

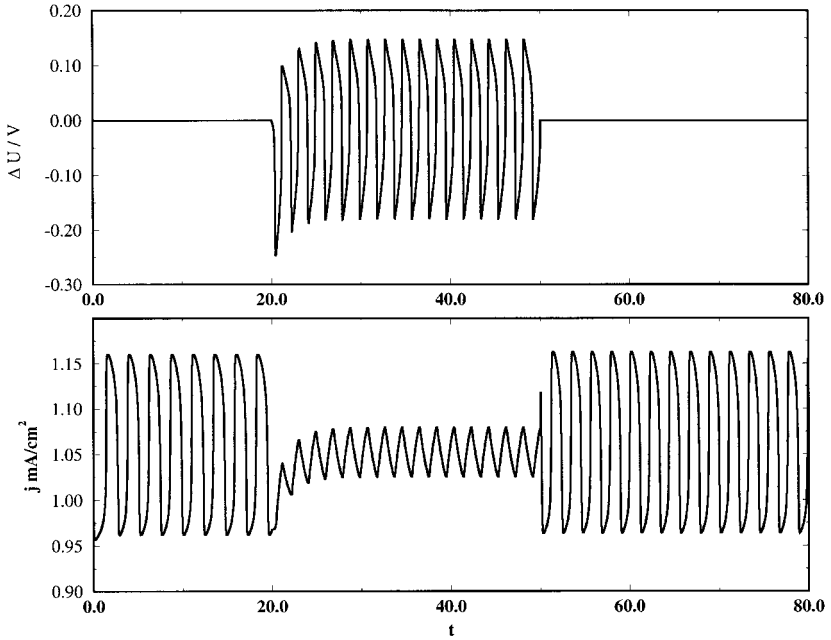

Figure 7-5: Numerical derivative feedback control implemented in a potentiostatic three-variable H_2 oxidation model [26]. Fig. a) and Fig.b) show the evolution of the applied variations ΔU in the control parameter U_{ex} (control signal) and the total current density, respectively. Control is applied at time t=20 and turned off at t=50. Numerical parameters: k_x =100; $c_{Cu} = 10^{-4}$; $c_x = 3 \times 10^{-3}$; U_{ex0} = 1560 mV/SCE; RA=1250Ωcm^2; control gain: α= -2000. For the formulation of the full model and the values of remaing parameter, see ref. [29, 26].

Moreover, both variable are seen to be strictly in phase. This behavior can be understood from eq. 7.11 and recalling that $j = (U_{ex} - \phi)/\rho$: Increasing values of the gain lead to an increasing resonant behavior of ϕ and U_{ex} since their time derivatives become more and more equal. In the limit of negative infinite gain, $\dot{\phi} = \dot{U_{ex}}$ and therefore $\dot{j} = 0$. Hence, the total current would be constant with ϕ and U_{ex} still exhibiting oscillations. This, of course, would not constitute the stabilization of an unstable steady state since j is not a system variable. At finite α, there is some finite $\dot{j}$ leading to small-amplitude oscillations.

7.4 $\dot{\theta}/I$-derivative control

7.4.1 Experimental results

Prior to the application of derivative feedback control the oscillatory $H_2/Cu/Br^-$-oxidation system was characterized by cyclic voltammetry using the RRDE. The ring was held at the contant potential $U_{ring} = +0.7V/Hg_2SO_4$ in order to monitor the

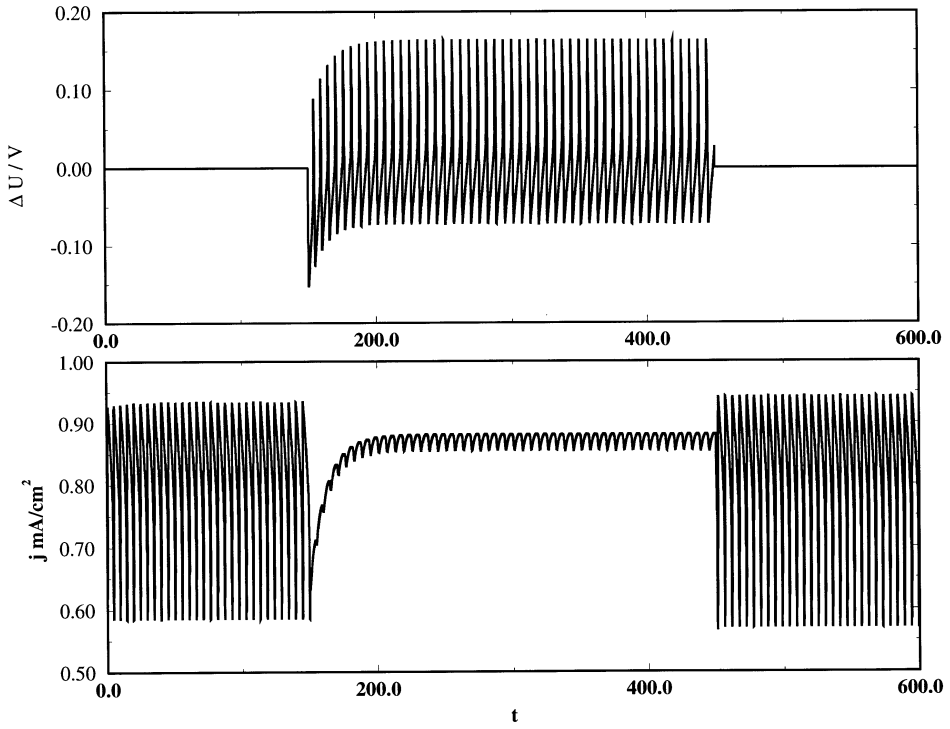

Figure 7-6: Effect of derivative feedback control in a potentiostatic formic acid oxidation model [72] . Control is applied at time $t = 150$ and switched off at $t = 450$. The time series show a) the control signal ΔU, b) the total current density j_{tot}, Numerical parameters: $pH = 1$; $U_{ex0} = 800$ mV/SCE; RA=437.5$\Omega\, cm^2$; $c_{FA} = 0.05$ mol/l; control gain: $\alpha = -5000$.

bromide oxidation. Fig. 7-8a and Fig. 7-8b show the I/U behavior of the ring current ΔI_{ring} and the disc current I, respectively. The ring current is plotted during the anodic scan only. Both currents are seen to exhibit correponding regular big-amplitude peaks interspersed with periodic small-amplitude peaks. At high potentials the surface becomes passivated due to the adsorption of oxygen-containing species [153, 98]. The black circle to the left of the CV-curve at a current of 0.1 mA indicates the value of the double layer potential ($\phi \approx -0.18$ V/Hg_2SO_4) of the stationary state of the system as obtained when correcting the outer applied potential ($\approx$+0.6 V/Hg_2SO_4) by the IR_{ex} drop neglecting the solution resistance.

Fig. 7-9, 7-10 and 7-11 show the time evolution of the ring current (upper graph in each partial figure) and disc potential (lower graph in each partial figure) when $\dot{\theta}_{Br^-}/I$- derivative control is applied during oscillatory H_2 oxidation under galvanostatic conditions (I=0.1 mA). At the outset of the time series of Fig. 7-9 the feedback control was off ($\alpha = 0$, see period denoted "a"). Upon increasing the control gain

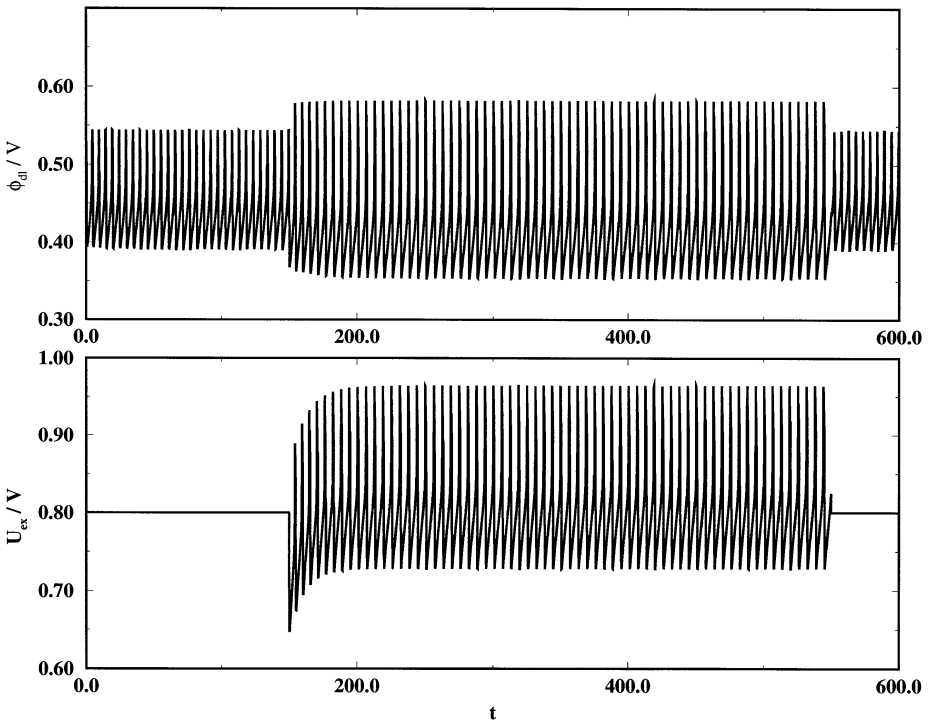

Figure 7-7: Effect of derivative feedback control in a potentiostatic formic acid oxidation model [72]. Control is applied at time $t = 150$ and switched off at $t = 450$. The time series show a) the double layer potential ϕ_{dl} vs. SCE, b) the instantaneous outer potential $U_{ex} = U_{ex0} - \alpha dj/dt$ vs. SCE. Numerical parameters as in previous figure.

to $\alpha = +2.0$ (period "b") the amplitude of the period-1 potential oscillations is seen to decrease. For $\alpha = +3.0$ (period "c" and "d"), finally, one recognizes a dramatic decrease of the amplitude of the potential oscillations followed by the successful stabilization of an stationary state at a double layer potential $\phi \approx$-0.18V/Hg_2SO_4 is observed. Simultaneously, the oscillations in the ring current disappear. The stationary potential compares favorably with that obtained from the IR correction above confirming successful control. After control had been switched off (period "e"), the stabilized stationary system relaxed back to the original oscillatory regime. Time period "e" and "f" ($\alpha = +3.0$) show that the system could be reproducibly brought back on the previously unstable stationary state by increasing α. Fig. 7-10 and 7-11 indicate the possibility for the H2 oxidation system to be stabilized on the same stationary state even for more complex uncontrolled periodic regimes. In the former figure very small periodic modulation of the stabilized state ($\alpha = +1.0$) is observed due to intrinsic perturbations. Moreover, at the outset of period "b" it is clearly seen

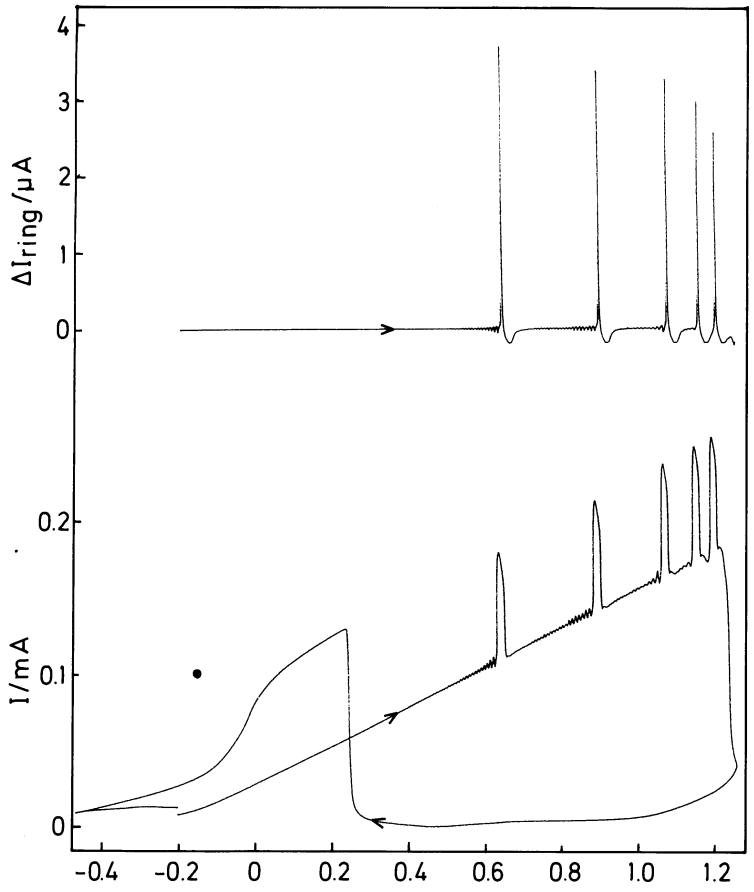

Figure 7-8: Cyclic voltammetry of the oscillatory H_2 oxidation system using a rotating-Au ring-Pt disc-electrode. Upper part: ring current corresponding to $2Br^- \longrightarrow Br_2 + 2e^-$ relative to the stationary ring current, $U_{ring} = +0.7$ V/Hg_2SO_4. Lower part: total current vs. outer applied potential U_{ex}. Experimental parameters: $R_{ex}A = 875\ \Omega cm^2$,scan rate=5 mV/s, 2000 rpm, 6×10^{-5} mol/l Cu^{2+}; 10^{-5} mol/l Br^-; 0.5 mol/l H_2SO_4

how the system gradually spirals in toward the final stationary point. In the latter figure, in contrast, where α was chosen to be +2.0, the stronger feedback control acted immediately on the system and no discernible spiralling could be observed prior to the stationary behavior. It is crucial to note for the further discussion that the positive values of α necessary for successful control correspond to a negative global feedback control according to eq. 7.1.

Next, the ring potential was lowered to $U_{ring} = -0.62$ V/Hg_2SO_4 in order to monitor the reduction current of copper ions at the ring and thereby the change of coverage of copper on the disc. Fig. 7-12 shows the observed behavior of the ring

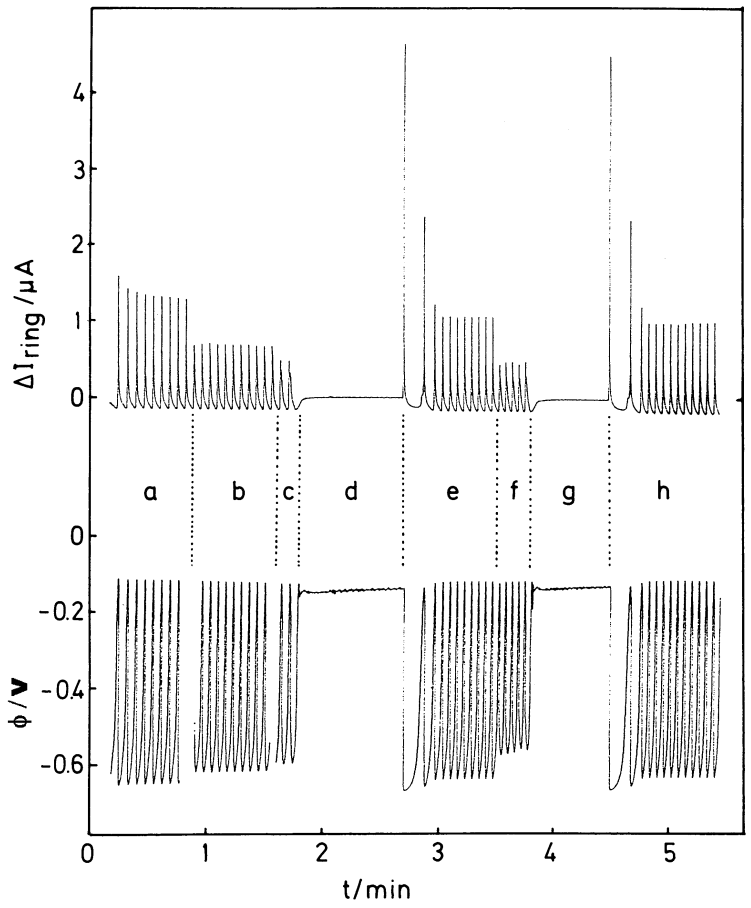

Figure 7-9: Stabilization of an unstable stationary state by means of $\dot{\theta}/I$ derivative (negative) feedback control during galvanostatic potential oscillations in the H_2 oxidation system at a RRDE. $I = 0.1$ mA, other conditions and reference electrode as in Fig. 7-8. The upper and lower graph show the time evolution of the ring-current and the disc potential, respectively.
gain values α: a,e,h:$\alpha = 0.0$; b: $\alpha = 2.0$, c,d,f,g:$\alpha = 3.0$.

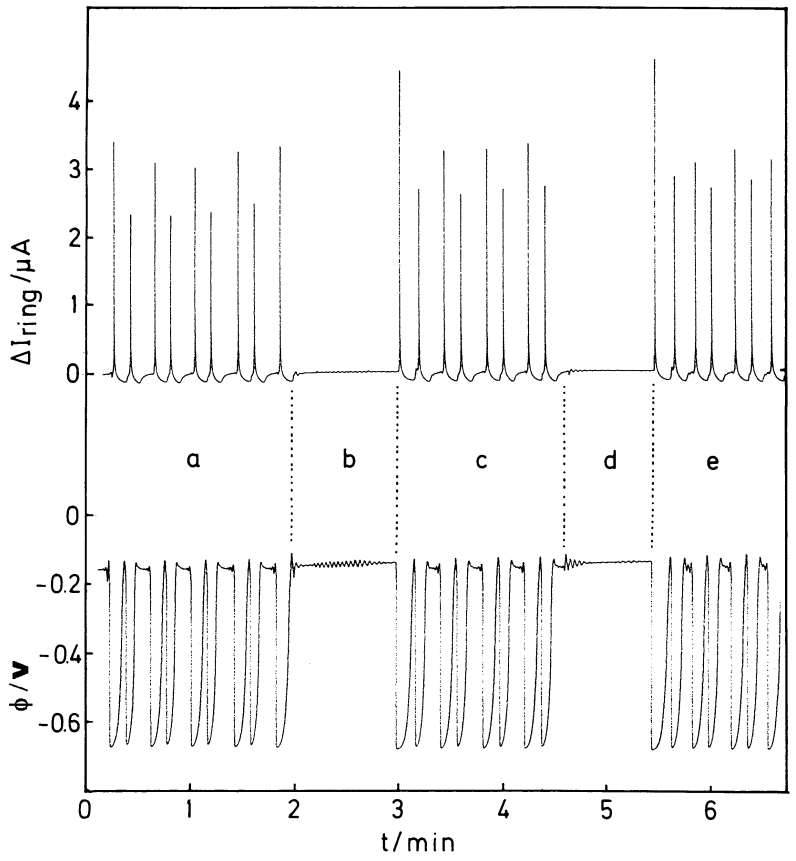

Figure 7-10: Stabilization of an unstable stationary state by means of $\dot{\theta}/I$ derivative (negative) feedback control during galvanostatic potential oscillations in the H_2 oxidation system at a RRDE. $I = 0.1$ mA, other conditions as in Fig. 7-9. The upper and lower graph show the time evolution of the ring-current and the disc potential, respectively.
gain values α: a,c,e:$\alpha = 0.0$; b,d: $\alpha = 1.0$.

current and disc potential under uncontrolled and controlled conditions (80 - 115 s,α =+3.0). The ring current is plotted in absolute figures with $I_{ring,0}$ being -0.15 μA. The pronounced positive peaks of ΔI_{ring} in the ring signal indicate considerable amounts of copper deposited and dissolved during oscillations. Although a complete stabilization of the unstable stationary state could not be achieved even for large positive gains, the amplitude of the potential oscillations was clearly reduced. Note that in contrast to $\dot{\theta}_{Br^-}$/I control, a positive feedback was required for reduction of amplitude during $\dot{\theta}_{Cu}$/I control. Conversely, in Fig. 7-13 and 7-14 negative values of α were applied during both control methods. One recognizes that inverse feedback

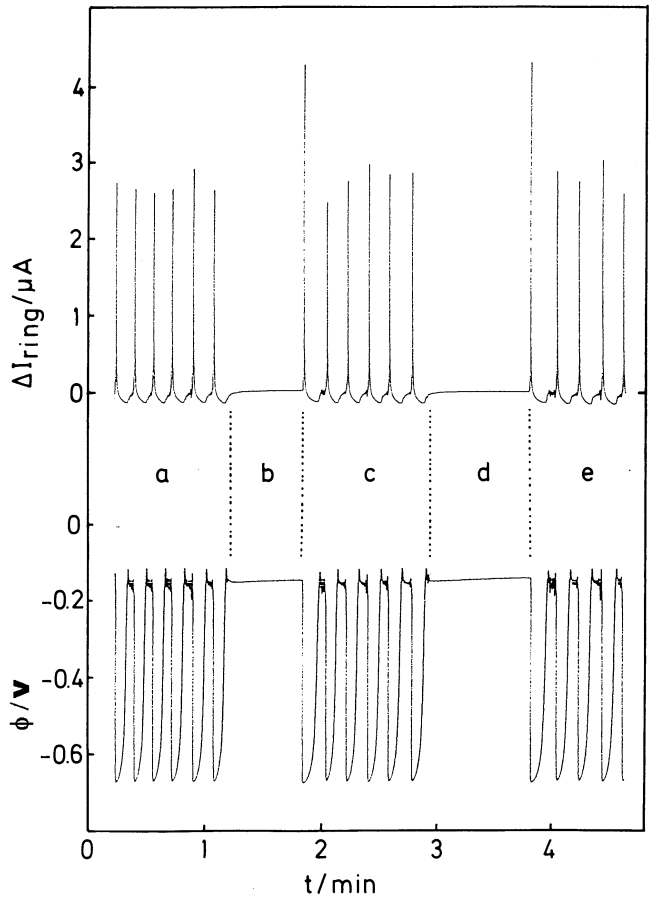

Figure 7-11: Stabilization of an unstable stationary state by means of $\dot{\theta}/I$ derivative (negative) feedback control during galvanostatic potential oscillations in the H_2 oxidation system at a RRDE. I = 0.1 mA, other conditions as in Fig. 7-9. The upper and lower graph show the time evolution of the ring-current and the disc potential, respectively.
gain values α: a,c,e:α = 0.0; b,d:α = 2.0.

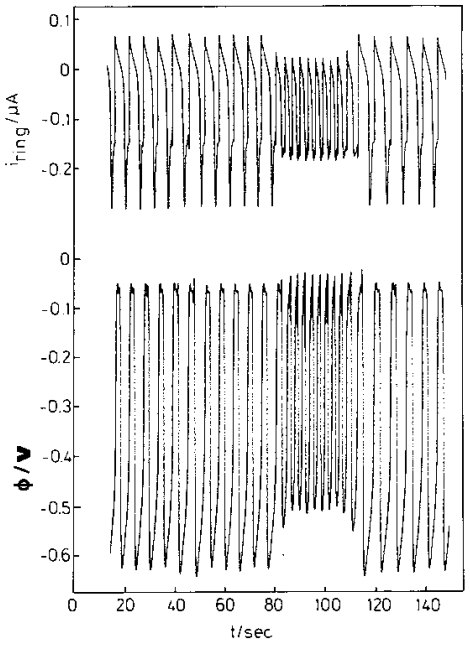

Figure 7-12: Effect of $\dot{\theta}/I$ derivative (positive) feedback control during galvanostatic potential oscillations in the H2 oxidation system at a RRDE. $I = 0.08$ mA, $U_{ring} = -0.62$ V /Hg_2SO_4. At the ring electrode copper ions are reduced according to $Cu^{2+} + 2e^- \longrightarrow Cu$. The upper and lower part depict the time evolution of the ring current and of the disc potential, respectively. Control was applied at $t \approx 80s$. Control gain $\alpha = +3.0$. Other parameters: 2000 rpm, 10^{-4} mol/l Cu^{2+}; 10^{-5} mol/l Br^-; 0.5 mol/l H_2SO_4, the potential is given vs. Hg/Hg_2SO_4.

(positive for $\dot{\theta}_{Br^-}/I$ control and negative for $\dot{\theta}_{Cu}/I$) leads to an increase in the potential amplitude indicating the wrong feedback sign for stabilization of the stationary point.

7.4.2 Model calculations

Linear stability analysis

Consider the electrochemical reaction scheme

$$X + * \overset{k_{a,x}(\phi),k_{d,x}(\phi)}{\rightleftharpoons} X_{ads} \tag{7.17}$$

$$Y + * \overset{k_{a,y}(\phi),k_{d,y}(\phi)}{\rightleftharpoons} Y_{ads} \tag{7.18}$$

$$Z + * \overset{k_r(\phi)}{\longrightarrow} P + ne^- \tag{7.19}$$

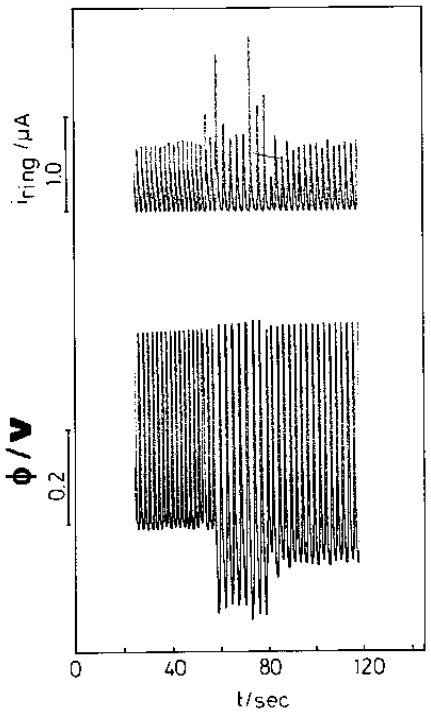

Figure 7-13: Effect of $\dot{\theta}/I$ derivative feedback control during galvanostatic potential oscillations in the H_2 oxidation system at a RRDE for inverse control gains.
Positive $\dot{\theta}_{Br^-}/I$ feedback control, upper and lower parts show ring current and disc potential, respectively. $I = 0.25mA, U_{ring} = +0.7V/Hg_2SO_4, \alpha = -1.0$. Control was applied at $t \approx 55s$. Other parameters as in Fig. 7-12.

with the notations as in model 7.2,7.3 and with Y denoting an additional fast chemical species. The given model is essentially the 3-variable version of model 7.2,7.3 for the description of electrochemical HNDR oscillators with a nonessential species providing the faradaic current.

Transforming the given reaction scheme into a dimensionless mathematical model of the essential variables θ_X and θ_Y and ϕ under galvanostatic conditions, one obtains

$$\dot{\theta_X} = f(\theta_X, \theta_Y, \phi) \tag{7.20}$$

$$\dot{\theta_Y} = g(\theta_X, \theta_Y, \phi) \tag{7.21}$$

$$\epsilon\dot{\phi} = j - h(\theta_X, \theta_Y, \phi) \tag{7.22}$$

with the function f and g modelling the adsorption and desorption of the chemical species X and Y, respectively; again, h represents the rate expression of the faradaic current (current carrier) of the system. The parameter j denotes the total current

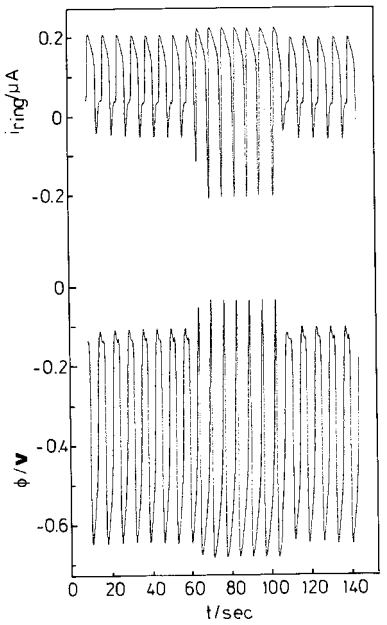

Figure 7-14: Effect of $\dot{\theta}/I$ derivative feedback control during galvanostatic potential oscillations in the H_2 oxidation system at a RRDE for inverse control gains. Negative $\dot{\theta}_{Cu}/I$ feedback control; upper and lower part show absolute ring current and disc potential, respectively. $I = 0.08$ mA, $U_{ring} = -0.62$ V $/Hg_2SO_4, \alpha = -1.22$. Control was applied at $t \approx 65s$. Other parameters as in Fig. 7-12

density which is used as control parameter during $\dot{\theta}/I$ control. In contrast to the 2-variable version, the function h is not assumed to exhibit a region of HNDR since this is taken care of by the additional third fast variable. The parameter ($\epsilon << 1$) denotes a relative time scale of the dynamics of ϕ and of the slow chemical species.

In order to model the experimental electrochemical H_2 oxidation system, an anodic current- carrying reaction is assumed. Moreover, the stationary θ_X/ϕ (θ_Y/ϕ) characteristics are assumed to show a negative (positive) slope what corresponds to the electrosorption behavior of Cu^{2+} (Br^-). From these assumptions the following relations result for the Jacobian matrix elements evaluated at the stationary state:

$$f_{\theta_X} < 0, f_{\theta_Y} < 0, g_{\theta_X} < 0, g_{\theta_Y} < 0, f_\phi < 0, g_\phi > 0, h_{\theta_X} < 0, h_{\theta_Y} < 0, h_\phi > 0$$

Consequently, the sign pattern of the Jacobian J reads

$$\begin{pmatrix} - & - & - \\ - & - & + \\ + & + & - \end{pmatrix}$$

For the characteristic polynom of the 3-Variable model (eq. 7.20-7.22) it follows

$$\begin{aligned} Det\,|\lambda I - J| &= \lambda^3 - TrJ\lambda^2 + \\ &(f_{\theta_X} g_{\theta_Y} - g_{\theta_X} f_{\theta_Y} + f_{\theta_X} h_\phi + h_{\theta_X} f_\phi + g_{\theta_Y} h_\phi + h_{\theta_Y} g_\phi)\lambda - DetJ \\ &= \lambda^3 + a\lambda^2 + b\lambda + c \end{aligned} \tag{7.23}$$

where λ denotes the eigenvalues of the system. Using the Routh-Hurwitzt-criterion for the solution behavior of polynomials [195], it can be shown that for sufficiently high values of g_ϕ parameter b becomes always negative with c remaining positive. This is a sufficient condition for the existence of two complex eigenvalues with positive real part as well as one negative real eigenvalue. Therefore, for large g_ϕ, i.e. for fast adsorption and desorption of Y, the stationary state is a unstable focus leading to sustained potential oscillations.

In the more special case of a diffusion limited current-carrying reaction, as found in the H_2 oxidation under fast stirring [29], the Jacobian at the steady state simplifies further yielding the pattern

$$\begin{pmatrix} - & - & - \\ - & - & + \\ + & + & 0 \end{pmatrix}.$$

Now, parameter c in the characteristic equation becomes $c = -DetJ = -h_{\theta_X} k_{d,y}(\phi) f_\phi - h_{\theta_X} k_{d,x}(\phi) g_\phi$. For sufficiently large g_ϕ, c is seen to be positive with $a > 0$ and $b < 0$ leading to a Hopf bifurcation [195]. In the following it is assumed that the model parameters are chosen such that sustained limit cycle osillations occur under uncontrolled conditions.

$\dot{\theta}_Y/I$ feedback derivative control

In contrast to the previously described $\dot{I}/U$-derivative control method, the control signal $\alpha\dot{\theta}_Y$ is not a function of the control parameter j. Consequently, the control becomes simply additive. The controlled system equations read

$$\dot{\theta_X} = f(\theta_X, \theta_Y, \phi) \tag{7.24}$$

$$\dot{\theta_Y} = g(\theta_X, \theta_Y, \phi) \tag{7.25}$$

$$\epsilon\dot{\phi} = j - h(\theta_X, \theta_Y, \phi) + \alpha\dot{\theta}_Y. \tag{7.26}$$

The parameters of the characteristic equation of the controlled system $\lambda^3 + a\prime\lambda^2 + b\prime\lambda + c\prime = 0$ read

$$a\prime = -\left(f_{\theta_X} + g_{\theta_Y} + \alpha g_\phi\right) \tag{7.27}$$

$$b\prime = g_{\theta_Y} f_{\theta_X} - g_{\theta_X} f_{\theta_Y} + \alpha g_\phi f_{\theta_X} + h_{\theta_X} f_\phi - \alpha g_{\theta_X} f_\phi + h_{\theta_Y} g_\phi \tag{7.28}$$

$$c\prime = c_{uc} \tag{7.29}$$

where c_{uc} denotes the parameter c of the uncontrolled model.

In order for the control to stabilize the system on the unstable steady state, the following conditions must be fulfilled:

$$a\prime > 0\, b\prime > 0\, c\prime > 0 \tag{7.30}$$

$$a\prime b\prime - c\prime > 0 \tag{7.31}$$

From eq. 7.27 and 7.28 it is clear by inspection that the stability conditions can be met if α is chosen sufficiently negative, i.e. if a negative feedback control is applied.

$\dot{\theta}_X/I$ feedback derivative control

Next, the time derivative of the slower variable θ_X is used as control signal. Similarly to the preceeding paragraph, the evolution equation of variable ϕ of the controlled model system reads

$$\epsilon\dot{\phi} = j - h(\theta_X, \theta_Y, \phi) + \alpha\dot{\theta}_X. \tag{7.32}$$

For the parameter $a\prime, b\prime$ and $c\prime$ one obtains

$$a\prime = -\left(f_{\theta_X} + g_{\theta_Y} + \alpha f_\phi\right) \tag{7.33}$$

$$b\prime = g_{\theta_Y} f_{\theta_X} - g_{\theta_X} f_{\theta_Y} + \alpha f_\phi g_{\theta_Y} + h_{\theta_X} f_\phi - \alpha f_{\theta_Y} g_\phi + h_{\theta_Y} g_\phi \tag{7.34}$$

$$c\prime = c_{uc}. \tag{7.35}$$

Successful stabilization according to eq. 7.30 and 7.31 is only achievable if the control gain α is sufficiently positive implying a positive feedback control.

Numerical model calculations

In order to check the experimental and analytical results numerically, the $\dot{\theta}/I$ derivative feedback control as formulated in the previuos section was implemented in a three- variable model of the galvanostatic H_2 oxidation reaction proposed in ref. [29]. Fig. 7-15a and b represent the calculated time evolution of $-\dot{\theta}_{Br^-}$ and ϕ under $\dot{\theta}_{Br^-}/I$ control. After application of negative feedback control ($\alpha = -0.02$) the system spirals onto the stablized focus. As control is switched off ($t = 120$) the original limit cycle behavior restores. Similarly, in Fig. 7-16a and b it is portrayed that $\dot{\theta}_{Cu}/I$ derivative control succesfully suppresses the potential oscillations for positive feedback.

7.4.3 Distinction between HNDR oscillators with respect to the current carrier

The previous section showed that the sign of successful $\dot{\theta}/I$ feedback control depends characteristically on the sign of the off-diagonal element of the Jacobian describing the regulation of ϕ on $\dot{\theta}$ of the species used as control signal; note that this matrix element is linked to the role the species plays within the oscillatory mechanism. This finding can therefore be exploited for an experimental identification and distinction

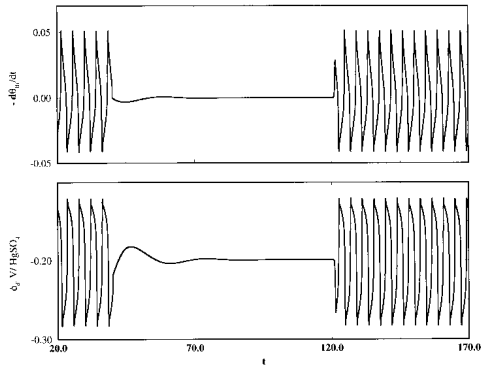

Figure 7-15: Numerical $\dot{\theta}_{Br^-}/I$ derivative negative feedback control implemented in a galvanostatic three-variable H_2 oxidation model [29]. The unstable stationary state is seen to be stabilized. Fig. a) and Fig.b) show the evolution of $-\dot{\theta}_{Br^-}$ (similar to upper graph of Fig. 7-10) and the double layer potential ϕ_{dl}, respectively. Control is applied at t=40 and turned off at t=120. Numerical parameters other than given in table 1 of ref. [29] are $c_{Cu^{2+}} = 10^{-4}$; $c_x = 4 \times 10^{-3}$; $j_{tot} = 0.5$ mA/cm^2; control gain: α= -0.02.

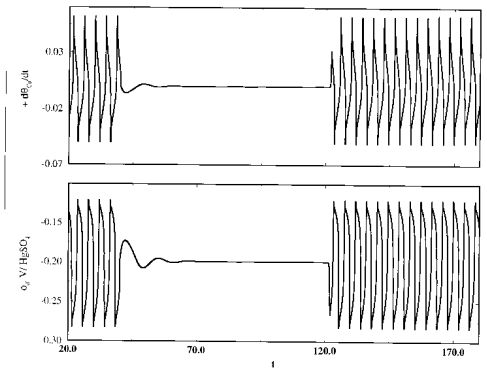

Figure 7-16: Numerical $\dot{\theta}_{Cu}/I$ derivative positive feedback control in the H_2 oxidation model [29]. The unstable stationary state is seen to be stabilized. Fig. a) and Fig.b) show the evolution of $\dot{\theta}_{Cu}$ (in correspondence to upper graph of Fig. 7-12) and the double layer potential ϕ_{dl}, respectively. Control is applied at t=40 and turned off at t=120. Control gain: α= +0.01. All other numerical parameter values as in previous figure.

between oscillatory electrochemical mechanisms. Focus will be on the experimental identification of 2- variable prototype models appropriately describing the Jacobian sign pattern of an unknown electrochemical HNDR oscillators.

Two classes of oscillatory models with HNDR were described in literature. First, there are models for the description of systems such as the H_2 oxidation [29, 26] or formic acid oxidation where the faradaic current is provided by a nonessential species (see model 7.2,7.3 and 7.17-7.19); consequently, it does not affect the coverages of the essential chemical species. In the case of an anodic faradaic current, the aforementioned 3-variable HNDR oscillator with a nonessential current-carrying species can be reduced to a 2-variable model of θ_X and ϕ by adiabatic elimination of θ_Y yielding an oscillatory model (similar to model 7.4-7.5) with the following Jacobian sign pattern under oscillatory conditions

$$\begin{pmatrix} - & - \\ + & + \end{pmatrix}.$$

Second, Koper and Sluyters [64] reported on a class of galvanostaticly oscillatory 2-variable models which represent an extension of simplier models for the description of the oscillatory electrochemical reduction of metal ion in the presence of catalysts. A negative impedance originating chemically from the fast adsorption and desorption of a catalyst was included in the functional form of the rate constant $k_r(\phi)$ of the current-carrying reaction. In the extended type of model, a potential dependent adsorption and desorption of the slow chemical species was shown to lead to an HNDR and consequently to galvanoststic oscillations. Although there is no experimental example so far for a galvanostatic oscillator of this type, the existence of such oscillators is well feasible from a chemical point of view. The model which consisted of the evolution equations of a slow chemical variable θ and the fast autocatalytic ϕ reads

$$\dot{\theta} = k_a(\phi)(1-\theta) - k_d(\phi)\theta - k_r(\phi)\theta \tag{7.36}$$

$$\epsilon\dot{\phi} = j - k_r(\phi)\theta \tag{7.37}$$

where j, k_a, k_d, k_r are the applied current density and the rate constants of adsorption, desorption and reaction, respectively. As in eq. 7.26 ϵ denotes the relative time scale of the two variables. Due to its galvanostatic oscillations, the extended model was considered to fall into the same category in terms of the destabilizing mechanism as the H_2 or FA system. However, mechanistically there is a considerable difference between both types of galvanostatic models insofar as in the latter model-type the reaction providing the faradaic current is directly consuming the slow chemical species. The current-carrying species is consequently an essential one, in contrast to the aforementioned type of HNDR oscillators where it was nonessential. This results in a different 2×2 Jacobian sign pattern under oscillatory behavior:

$$\begin{pmatrix} - & + \\ - & + \end{pmatrix}$$

It is important to note that a distinction between the two types of Jacobian sign patterns by impedance spectroscopy is impossible since impedance values are functions of all (in the case of a 2-variable model) four Jacobian elements. The $\dot{\theta}/I$ derivative feedback control method using the slow chemical species, in contrast, is capable to determine the off diagonal element and can therefore be used to determine the appropriate skeleton mechanism. Applying the $\dot{\theta}/I$ derivative feedback control to a HNDR oscillator corresponding to the latter class (current carriying species essential) would require a negative feedback for a successful suppression of oscillations whereas the former class of HNDR models (current-carrying species nonessential) required a positive feedback.

7.5 Discussion

$\dot{I}/U$ derivative feedback control

The dynamic response of electrochemical HNDR oscillators under $\dot{I}/U$ derivative control action has been studied in model and experiment. $\dot{I}/U$ control was unable to stabilize an unstable stationary point in the systems under consideration. More generally, the linear stability analysis given in section 3 indicated that whenever ϕ is time dependent under oscillatory conditions, i.e. when the ohmic resistance ρ is not negligible, the $\dot{I}/U$ derivative feedback technique must fail to stabilize a stationary state. Conversely and more importantly, successful suppression of oscillations by means of $\dot{I}/U$ control for the limiting case where ρ is neglibgible definitely proves that ϕ is quasiconstant under oscillatory conditions which, in turn, is a sufficient condition for a truly potentiostatic oscillator. Note that knowledge of the actual solution resistance is irrelevant. These results suggest the following operational procedure for the identification of a truly potentiostatic oscillator: The ohmic resistance should be reduced repeating the control test until either the uncontrolled systems stops to be oscillatory and ϕ is proved to be essential or the suppression of oscillations is successful upon control and the instability is proved to be of chemical nature.

In ref. [105] the effect of $\dot{I}/U$ control during the potentiostatic electrodissolution of Cu in acetic acid/acetate buffer (AAB) was desribed. In Fig. 7 of ref. [105] (reproduced in Fig. 7-17) the authors report on the successful suppression of current oscillations upon $\dot{I}/U$ feedback control associated with a vanishing control signal. The suppression of oscillations was found for all gains beyond a critical value. According to the present study, the findings strongly suggest for the Cu/AAB system to be an example of a truly potentiostatic oscillator where ϕ is nonessential despite an electron transfer step involved.

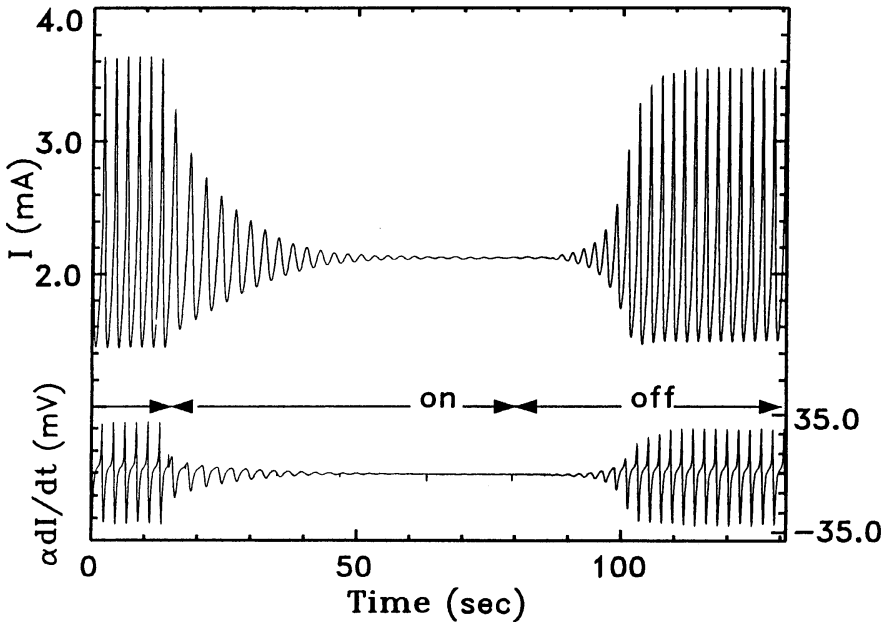

Figure 7-17: $\dot{I}/U$ Derivative control in the oscillatory Cu/acetate system without external resistance, adopted from ref. [105].

$\dot{\theta}/I$ derivative feedback control

Stabilization of unstable stationary states

The successful experimental suppression of potential oscillations in favor of a stationary point in an electrocatalytic system has been achieved by $\dot{\theta}_{Br^-}$/I negative feedback control. The stabilization has been shown to be reproducible and quite robust to system perturbations (see Fig. 7-10). The control signal has been obtained experimentally exploiting the properties of the ring currents of RRDEs. Of course, other in situ probes for the coverage of adsorbed species essential for the dynamics could be used if their response times are sufficiently short. In contrast to proportional feedback control [200, 206], the applied derivative control technique requires no *a priori* knowledge of the operating system in order to stabilize an intrinsic stationary state without offset.

Suppression of oscillations in chemical systems can be of practical importance where periodic reaction rates are undesirable due to unfavorable system characteristics. In the case of electrocatalytic systems, for instance, the repeated ad-and desorption of oxygen containing species on the electrode at an average current density contributes to a faster degradation of the electrode material, e.g. due to roughening, than observed for the corresponding stationary current associated with an intermediate oxygen coverage. Moreover, control techniques offer the possibility to extend the

stability region and therefore the region of possible operating points.

The stabilization of an unstable stationary point by $\dot{\theta}_{Cu}$/I control was not completely achieved even for large values of the control gain. There are two reasons for this finding: First, the proper synchronization of the control action is disturbed due to periodic bulk deposition of Cu [75]. Deposition and Dissolution of bulk copper is obviously monitored by the ring current, while only the first layer affects the dynamics of the oscillator due to site blocking. Second, a slow drift of the stationary ring current $I_{ring,0}$ impedes the precise measurement of ΔI_{ring} over a long time interval. However, the decrease in oscillations amplitude upon control (Fig. 7-12 in contrast to the incorrect feedback sign used in Fig. 7-13 and Fig. 7-14) uniquely indicates the "correct" sign of the feedback required for successful control.

Experimental identification of suitable oscillatory models and role of species

It is crucial to realize that the type of feedback necessary for the stabilization of the unstable stationary point is not arbitrary but is directly related to the mechanistic role of the species monitored at the ring electrode. In particular, the stability analysis of section 4 clearly illustrates that the off diagonal Jacobian elements $f_\phi = \partial\dot{\theta}_X/\partial\phi$ ($g_\phi = \partial\dot{\theta}_Y/\partial\phi$) determines the correct sign of the $\dot{\theta}_{Cu}$ ($\dot{\theta}_{Br^-}$) derivative feedback. Therefore, control experiments can provide useful mechanistic information on the experimental system. Despite its practical importance, this aspect of chemical control experiments has never been discussed before.

The category of electrochemical oscillators characterized by an HNDR and ϕ being essential [27, 74] has been further refined into two subcategories depending whether or not the current carrier (main current providing reaction) is provided by the slow essential chemical species; accordingly, the current carrier was termed "dependent" and "independent", respectively. Due to the distinct Jacobian matrix element $\partial\dot{\theta}/\partial\phi$ of the corresponding prototype models, derivative control can be used for a clear identification of the appropriate subcategory associated with a prototype model for the oscillator under investigation. Note that for this purpose the knowledge of the essential chemical species is required which in many cases can be obtained from chemical intuition. Conversely, with the knowledge whether the current carrier is dependent or independent, one can identify those chemical species which show the approporiate feedback signs for successful control and therefore are possible candidates for the slow essential variable; likewise candidates for the fast chemical species in the case of an independent current carrier are identified. Table 7.1 summarizes the required correct feedback sign for the respective cases. The latter method can drastically reduce the number of possible species eligible for an appropriate kinetic model.

7.6 Summary

An experimental feedback control test for a truly potentiostatic oscillator was introduced. It can easily be applied to electrochemical oscillators whose mechanistic basis of the instabiliy is unknown, but possibly involves ϕ as a nonessential variable [76, 67, 77, 78]. Moreover, a second experimental test was presented which allows a

	current-carrying species essential	**current-carrying species nonessential**
anodic current carrier	$\begin{pmatrix} - & + \\ - & + \end{pmatrix}$ $\dot{\theta}_{slow}$/I : negative feedback	$\begin{pmatrix} - & - & - \\ - & - & + \\ + & + & 0 \end{pmatrix}$ $\dot{\theta}_{slow}$/I : positive feedback $\dot{\theta}_{fast}$/I : negative feedback
cathodic current carrier	$\begin{pmatrix} - & - \\ + & + \end{pmatrix}$ $\dot{\theta}_{slow}$/I : positive feedback	$\begin{pmatrix} - & - & + \\ - & - & - \\ - & - & 0 \end{pmatrix}$ $\dot{\theta}_{slow}$/I : negative feedback $\dot{\theta}_{fast}$/I : positive feedback

Table 7.1: Summary of the Jacobian sign patterns of model eq. 7.36 -7.37 and eq. 7.20-7.22 and the required feedback sign of the $\dot{\theta}$/I derivative control for successful suppression of oscillations for the subcategories of the HNDR oscillators according to the nature of the current carrier. In the case where the current-carrying species is nonessential, diffusion limited conditions are assumed leading to the zero element (see section 4). A finite potential dependence would not affect the required feedback signs.

further subclassification of HNDR oscillators with respect to the nature of the current providing species. Both subcategories are associated with suitable simple kinetic models. In combination with other techniques for the mechanistic identification of electrochemical oscillators such as impedance spectroscopy[23], both experimental tests can result in an operational method for a systematic clarification of the relevant dynamical processes of an unknown electrochemical oscillator as will be outlined in chapter 9.